Estuarine, Coastal and Shelf Science 274 (2022) 107926

Contents lists available at ScienceDirect

Estuarine, Coastal and Shelf Science

journal homepage: www.elsevier.com/locate/ecss

Sedimentological archives of coastal storms in South-West Wales, UK

Alexander Jardine[a,*], Katherine Selby[a], Ian W. Croudace[b], David Higgins[c]

[a] Department of Environment and Geography, University of York, York, YO10 5NG, United Kingdom
[b] Ocean & Earth Science, University of Southampton, National Oceanography Centre, Southampton, SO14 3ZH, United Kingdom
[c] School of English, University of Leeds, Leeds, LS2 9JT, United Kingdom

ARTICLE INFO

Keywords:
Storm surge
Saltmarsh
Sedimentology
Coastal storm
Saltmarsh sustainability

ABSTRACT

High magnitude coastal storms have persistently threatened human communities and environments. In the British Isles their frequency and magnitude are predicted to increase in the future with advancing climate change. This study analyses sedimentological evidence from south-west Wales to assess the impacts of high magnitude coastal storms in vulnerable coastal saltmarshes in the Three Rivers Estuarine Complex, Carmarthen Bay. Storm surge saltmarsh deposits were identified following geochemical and particle size analyses and dated using radionuclides ^{137}Cs and ^{210}Pb. The sedimentological evidence is compared with regional tidal gauge and meteorological records to assess variability in storm recording and corroborate the storms which produced the sedimentological deposits. Three episodes of high magnitude saltmarsh storm surge deposition are identified in 1954, 1977 and 1981. Evidence of storm erosion or alternative forms of storm deposition were not present. The sedimentological evidence highlights the comparative rarity of major depositional events in the saltmarshes between 1929 and 2019. The recorded depositional events combined with organic accretion have contributed to maintaining saltmarsh elevation relative to sea level.

There remains uncertainty surrounding the storm impacts on the saltmarshes of the Three Rivers Estuarine Complex. When the future 21st century threats of increasing regional atmospheric storminess and sea level rise are considered along with predictions of saltmarsh degradation, this study suggests further research is required to explore the sedimentological storm impacts. This could contribute to sustaining the vulnerable coastal saltmarsh environments and the important ecosystem services they provide.

1. Introduction

Coastal storms represent major hazards that are predicted to increase in frequency and magnitude with climate change (Haigh et al., 2016; Palmer et al., 2018). The United Kingdom Climate Projections 2018 (UKCP18) indicate sea level rise coupled with increasing atmospheric storminess will lead to greater detrimental impacts on coastal populations and environments (Burden et al., 2020; Lowe et al., 2018). As the threat of storms increases with climate change it is important to understand how coastal storms have impacted valuable coastal environments and appraise how these impacts may change in the future (Slingo et al., 2014; Dawson et al., 2016; Lowe et al., 2018).

In Great Britain, climatic change is predicted to cause coastal saltmarsh loss to increase with a >80% probability of saltmarsh retreat, under the most likely IPCC Representative Concentration Pathway (RCP) 8.5 scenario (most similar to Shared Socioeconomic Pathways (SSP5) 8.5 in IPCC AR6) by 2100 (Horton et al., 2018; Schwalm et al., 2020; Chen et al., 2021). The increasing frequency of high magnitude storms and sea level rise (SLR) could result in the degradation of valuable coastal environments which provide ecosystem services including blue carbon storage and sequestration, as well as coastal defence (e.g. Craft et al., 2009; Pendleton et al., 2012; Morris et al., 2018). Saltmarsh sediments also provide valuable records of environmental change including storm surges (Pilarczyk et al., 2014; Bunzel et al., 2021). Saltmarsh storm evidence can range from the deposition of coarse sediment horizons, sporadic deposition of discrete very coarse material (namely granules and pebbles) or the creation of erosional contacts depending on the life cycle of the storm energy-sediment interaction (Leonardi et al., 2018).

This multidisciplinary study investigated the impacts of coastal storms in south-west Wales where SLR and increasing atmospheric storminess are predicted to increase human and coastal environmental storm exposure (Palmer et al., 2018; Resources Wales, 2020). The study focuses on the sedimentological impact of coastal storms in the short

* Corresponding author.
E-mail address: apj518@york.ac.uk (A. Jardine).

https://doi.org/10.1016/j.ecss.2022.107926
Received 25 October 2021; Received in revised form 28 February 2022; Accepted 30 May 2022
Available online 1 June 2022

term from 1929 (oldest radionuclide date) to 2019 (data retrieved) and considers future impacts up to 2100. In the region, saltmarshes are predicted to achieve the >80% retreat probability as early as 2060 (Horton et al., 2018) while nationally significant infrastructures such as the Hinkley Point C nuclear power plant and Port of Milford Haven could be vulnerable (Lyddon et al., 2017; Poo et al., 2021).

Sedimentological evidence of storm surges in the Three Rivers Estuarine Complex, Carmarthen Bay enables the impact of coastal storms on the saltmarsh environment to be assessed. Regional tidal gauge data from Newlyn (1915–1961) and Milford Haven (1961–2020) enable an assessment of storm surge and sedimentological correspondence. Meteorological data from the Meteorological Office station at Pembroke, south-west Wales (1861–2020) allows further correspondence analysis between the meteorological and sedimentological data. This combination of sedimentological, tidal gauge and meteorological evidence is used to assess the impacts of coastal storms on a vulnerable saltmarsh environment between 1929 and 2021. The findings are considered along with future predictions of regional sea level rise and storminess until 2100 to appraise the future saltmarsh sustainability.

2. Materials and methods

2.1. Study location

2.1.1. Background and rationale

The research focussed on 189 km of coastline between Port Eynon, Swansea to Marloes Head, Pembrokeshire (Fig. 1(i)). This area includes Carmarthen Bay which covers an area of 661.2 km^2 at mean high water (MHW). The region includes the Three Rivers Estuarine Complex Special Area of Conservation and Milford Haven, an important port (Port of Milford Haven, 2016).

Generalised Pareto Distribution (GPD) storm models indicate that a

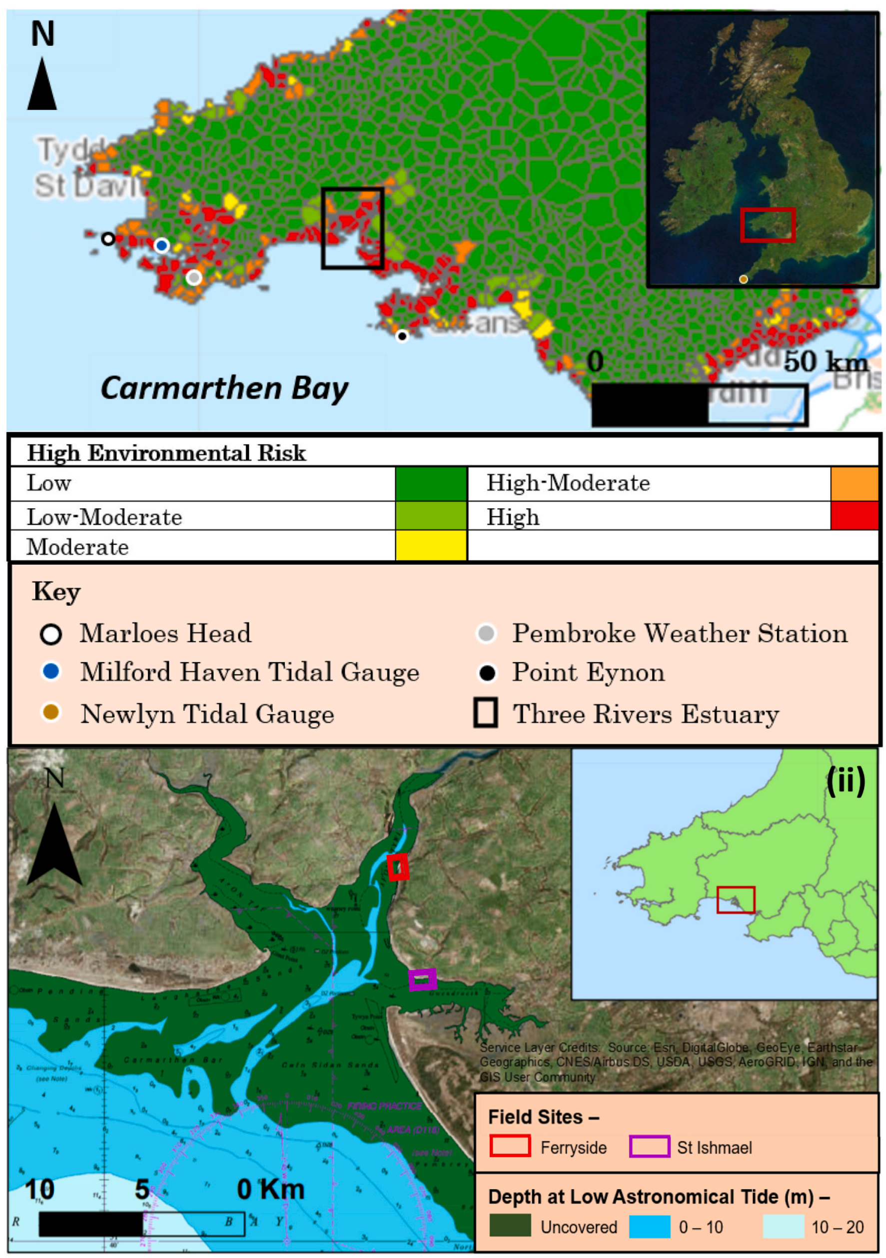

Fig. 1. (i-ii). (i) Study sites and areas exposed to high risk coastal flooding in 2020. (ii) Location of field sites in the Three Rivers Estuarine Complex, Carmarthen Bay. Depth at Lowest Astronomical Tide (LAT) highlights maximum tidal range and main channels. (Source: Natural Resources Wales, 2020).

1-in-10 year storm (in 2019) from the South West is characterised by winds of 26.6 ms^{-1} producing waves of a height of 6.94 m in the centre of Carmarthen Bay (Bennett et al., 2019). Weather data (2021) from Pembroke Dock record that the average wind speed is greatest in December and January registering Beaufort Force 5 (30 kph) although the 90th percentile exceeds Beaufort Force 6 (45 kph). For eight months of the year westerly (WSW-WNW) and southerly (SSE-SSW) winds prevail for >60% of days (Modern-Era Retrospective analysis for Research and Applications, Version 2, 2021).

Present coastal flood risk in Carmarthen Bay is very high as Natural Resources Wales (2020) Flooding Vulnerability Model exhibits 36/55 of the defined coastal zones are exposed to the highest possible environmental risk (Fig. 1(i)). In the Three Rivers Estuarine Complex the 50–100 year coastal management policies are no active invention and hold the line (Phillips et al., 2012). The saltmarshes at Ferryside and St. Ishmael are located in areas where the policy is hold the line as they have a railway to landward which is protected by rock armour. Regional storm surge skew (maximum observed sea level – maximum predicted sea level), is also predicted to increase by 0.7 mm/yr by 2100 (1981–2000 baseline) according to the most realistic MPI-ESM-LR-RCA4 model (Palmer et al., 2018). Regional UKCP18 models also estimate a relative SLR of >0.7 m by 2100 under the most likely RCP 8.5 scenario (most similar to SSP5 8.5) (Palmer et al., 2018; Schwalm et al., 2020).

2.1.2. Sedimentology and geomorphology

The two field sites are located at Ferryside and St. Ishmael in the Three Rivers Estuarine Complex, Carmarthen Bay (Fig. 1(ii)). The estuarine complex comprises the estuaries of the Rivers Taf, Tywi and Gwendraeth which are characterised by sand and mudflats, saltmarshes and intertidal channels (Bennett et al., 2020).

The Ferryside and St. Ishmael sites are both located in saltmarsh environments in the Tywi and Gwendraeth estuaries respectively (see Fig. 1(ii)) and classified as at the greatest environmental risk of coastal flooding (Resources Wales, 2020). The dominant species *Spartina anglica* is partially responsible for rapid saltmarsh expansion and sediment accumulation in the estuarine complex, which has experienced little channel migration over the last *c.* 200 years (Bristow and Pile, 2003; Pye and Blott, 2009). Carmarthen Bay is influenced by Atlantic south-westerly swell waves and locally-generated wind waves which can catalyse geomorphological change during winter storms (Pye and Blott, 2009; Bennett et al., 2019). The bay is underlain by Carboniferous and Devonian limestones and sandstones while sand predominates on the seafloor (Cooper and McLaren, 2007; Countryside Council for Wales, 2009).

Site locations close to the main channels and below mean high water springs (4.10 mOD) (Carmarthenshire County Council, 2019) were selected as storm surge waves from the south-west would theoretically experience little dissipation at the estuarine mouth and propagate over the two sites (Möller et al., 2014; Rupprecht et al., 2017). This enhanced the likelihood of storm surges producing sedimentological evidence (Tsompanoglou et al., 2011; Hawkes and Horton, 2012).

2.2. Fieldwork

The saltmarsh stratigraphy was first tested using a gouge corer at 50 m intervals along two transects parallel to the shore in the lower-middle saltmarsh in the Three Rivers Estuarine Complex and the Loughor Estuary. The core position and elevation were obtained to a precision of ±5 mm using a differential Global Positioning System (dGPS) (Woodroffe et al., 2015). Stratigraphy was recorded using a modified Troels-Smith (1955) classification. This information was used to inform subsequent sampling sites at Ferryside and St. Ishmael. In February 2019 a Russian corer with a 0.07 m chamber diameter and 1 m length was used to extract nine representative sediment cores per site at 20 m intervals (3600 m^2 area) for laboratory analyses (Frew, 2014).

2.3. Laboratory analyses

2.3.1. Geochemical analysis

Geochemical analysis of the sampled cores was undertaken to identify storm surge proxy elements (Williams, 2009; Otvos, 2011). X-ray fluorescence (XRF) geochemical analyses were undertaken using the Itrax® core scanner (Croudace et al., 2006) based at the British Ocean Sediment Core Research Facility on five cores. The five selected cores contained abrupt sandy deposits at similar elevations within the stratigraphy. Due to the Itrax® measuring procedures, the focus was on the relative abundance of 7 indicator elements. Ba, Ca and Sr were used as reliable indicators of marine flooding and evidence of storm and tsunami events (e.g. Schlichting, 2000; Szczuciński et al., 2012; Goslin and Clemmensen, 2017). Si and K were indicators of the abundance of medium-coarse grained sand common in storm surge deposits (Williams et al., 2011; Chague-Goff et al., 2016). Zr was used to indicate a higher relative abundance of resistant or heavy minerals from an offshore marine environment (Dezileau et al., 2011; Tsompanoglou et al., 2011). Ti abundance (against Rb) was alternatively used to indicate a fluvial origin as high Ti can indicate terrigenous input (Font et al., 2013).

The geochemical data were normalised against lithophile Rb to enable elemental comparison due to its low environmental mobility and lack of anthropogenic enrichment (Kylander et al., 2011; Weltje et al., 2015). Ti was also used as an immobile element due to its abundance and biological inactivity (Löwemark et al., 2011; Weltje et al., 2015). The relative abundance of each element (i.e. indicator/Rb or Ti) were presented as natural log (ln) ratios for comparative purposes (Weltje and Tjallingii, 2008).

2.3.2. Particle size analysis

Particle size analyses (PSA) were undertaken on the five cores to establish the variability of particle size. A laser diffraction PSA was undertaken using a Malvern® Mastersizer 3000 enabling a precision of 1 mm to be achieved at a resolution of 2 cm throughout the core. The particle size analysis was cross-checked with the higher resolution geochemical particle size indicator elements to ensure no major changes in grain size were missed. The analyses produced three D-Values (D10, D50 and D90) giving the cumulative sample mass values for 10%, 50% and 90% (Blott and Pye, 2001). The particle size of the samples was categorised using the Wentworth (1922) classification.

2.3.3. Principal Component Analysis

Dimension reducing Principal Component Analysis (PCA) was undertaken using PAST® software to identify the main factors distinguishing the potential storm surge deposits. For comparison, all data relative to Rb and Ti were natural log (ln) transformed (Croudace and Rothwell, 2015). The independent influence of geochemistry as well as the combined influence of geochemistry and particle size were analysed.

2.3.4. Radionuclide dating

Pb-210 and ^{137}Cs radionuclide dating were undertaken to evaluate sediment accumulation rates of the storm surge deposits and the age of layers. Pb-210 potentially provides information up to the last ~100 years while ^{137}Cs profiles can provide temporal data from 1950-present based on anthropogenic inputs (Appleby, 2002; Croudace et al., 2012; Baskaran et al., 2014; Andersen, 2017).

Samples weighing >10g taken from 1 cm intervals were freeze-dried, placed in vials and gamma counted at GAU-Radioanalytical Laboratories for 100,000 s. Total ^{210}Pb and ^{137}Cs were measured using well-type HPGe gamma spectrometry systems. Sampling was undertaken at 4 cm intervals in each core. Excess ^{210}Pb ($^{210}Pb_{xs}$) was then determined using the constant rate of supply (CRS) model (Croudace et al., 2012). Sample $^{210}Pb_{xs}$ was calculated by subtracting a supported value of 0.01 Bq g^{-1} from total activity. The natural log of $^{210}Pb_{xs}$ was plotted against depth to produce an age-depth model and estimate sediment accumulation rates (SAR) and ages.

Cs-137 was used to identify chronological markers of key radionuclide events (e.g 1963 bomb pulse, Sellafield releases) consistently identified in UK western saltmarshes. Comparison of the ^{137}Cs chronology with major ^{137}Cs discharges from Sellafield (Gray et al., 1995; Tsompanoglou et al., 2011; Swindles et al., 2018) enabled the creation of age-depth models and calculation of independent SARs producing an overall age profile.

2.4. Tidal gauge data

To assess storm surge height correspondence, historical data concerning observed and predicted tidal heights were obtained. The observed tidal gauge data were collected from the Milford Haven (July 1961–December 2020) and Newlyn (April 1915–June 1961) tidal gauge records from the British Oceanographic Data Centre (BODC) as they provided the longest spatially relevant observations (BODC, 2021). Datum conversions and tidal information are shown in Table 1. The combined age range gave appropriate temporal coverage for the likely age of the Three Rivers Estuarine Complex sediments.

The maximum surge height was calculated by subtracting observed tidal elevations from predicted tidal elevation determined from a gauge-specific POLTIPS (Oceanographic Centre, 2021a) hindcast. The hindcast was undertaken for the exact time the observed measurement was taken which varied accordingly with measurement intervals over time. The variability in maximum storm surge height and recorded elevation was then assessed for storm events. The data were cross-checked with site-specific storm surge records of the greatest surges from the National Tidal and Sea Level Facility (National Tidal and Sea Level Facility, 2021) and British Oceanographic Data Centre (BODC, 2021) to ensure the calculated storm surge magnitudes were appropriate and there was relevant dataset correspondence. Baseline surge magnitude ≥0.76 m at Milford Haven and ≥0.29 m at Newlyn were determined. These heights were selected as they represented the top 1% storm surge maximum height thresholds for each site. The top 1% surges were focussed upon as this study appraises high magnitude saltmarsh storm surge inundation. The observed tidal height was also considered when appraising deposit and archival records as this influences sedimentological storm surge signatures.

2.5. Meteorological data

The study investigated storm frequency and magnitude recorded at the Pembroke Meteorological Office weather station. This initially concerned the period from 1861 (start of records) to 2020 as the meteorological analysis was undertaken before radionuclide dates were received. This time scale was appropriate given that previous research in the Three Rivers Estuarine Complex indicated that the saltmarsh sediments were deposited during this period (Pye and Blott, 2009). Regional storms were identified from daily newspapers reports and Meteorological Office weather observations found in newspapers in the British Library's digitised archives (GALE, 2021).

Meteorological data from Pembroke for wind speed (Beaufort Force), wind direction (22.5° compass bearing) and barometric pressure (mm Hg) were compiled. For the full period of meteorological recording (initially from 1861 as the deposit dates were not known) many of the archived windspeeds were only reported in Beaufort Force. This standardised unit was therefore used throughout for the purpose of consistency so some readings were converted into Beaufort Force on Excel®. The greatest mean hourly speed within each storm was recorded to gauge the maximum mean storm strength. This ensured that the data were not skewed by anomalous gusts and lulls, and accurately reflected storm magnitude. Data from Prawle Point (Plymouth) 184.2 km south-south-east were provisionally collected if there was an absence of data from Pembroke. A database of every reported storm was created. This database was used to assess all storms recorded within periods corresponding with the sediment radionuclide dating range of the saltmarsh deposits. Particular attention was paid to wind direction and strength as higher wind velocities from the SSE-WNW were most likely to result in storm sedimentological evidence due to the orientation and bathymetry of the estuarine complex.

Table 1
Tidal information (2020) and datum conversion table and at Milford Haven and Newlyn. (Sources: National Oceanographic Centre, 2021a, 2021b).

Site	Conversion - Admiralty datum (mAD) to Ordnance datum (mOD)	Mean Low Water Neap (mAD)	Mean High Water Spring (mAD)	Highest Astronomical Tide (mAD)
Newlyn	−3.05 m	2.08	4.37	6.16
Milford Haven	−3.71 m	2.49	5.31	6.92

2.6. Dataset correspondence

The correspondence analysis between the sedimentological, tidal gauge and meteorological results focussed on storms in the radionuclide age uncertainty ranges. Meteorological events were identified with wind magnitude and direction noted. Identified storm surges (top 1%) within the date range were then extracted from tidal gauge records. Meteorological records that did not correspond with any tidal gauge record were discarded as a high magnitude surge inundation would be required to produce major (>3 cm) sandy saltmarsh deposits (Tsompanoglou et al., 2011; Leonardi et al., 2018). The following factors were determined the most important as they had the greatest influence on the likelihood of storms to produce sedimentological deposits:

- Wind speed magnitude
- Wind direction
- Storm surge height
- Observed overall surge height

Observed overall surge height was deemed the most important factor as a surge must penetrate inland and inundate the saltmarsh to produce clear sedimentological evidence (Hawkes and Horton, 2012; Garzon et al., 2019; Moskalewicz et al., in press). Other spatially relevant sedimentological research was also considered. The discussion considers which storms most likely produced the identified sedimentological evidence and the potential future implications of storms on the saltmarsh environment.

3. Results

3.1. Sedimentological

3.1.1. Stratigraphy

At Ferryside the basal unit was comprised of fine silts and clays (Troels-Smith, 1955). An abrupt sandy layer containing calcareous fragments was found in all nine cores with cores FSE2 and FSE3 containing two layers (Fig. 2(a)). The Troels-Smith assessment indicated organic content increased in the surface horizons and a trend of gradual upward fining was observed. FSE3, FSC2 and FSW3 were selected for laboratory analyses as they possessed the clearest stratigraphic indication of potential storm surge evidence in the form of abrupt sandy deposits.

Seven St. Ishmael cores recorded organic clay-silt basal horizons whilst SIC2 and SIC3 had a coarser silt base. Large abrupt sand deposits >3 cm interspersed with silt layers were noted above the basal layer in seven cores (Fig. 2(b)). No evidence of minor deposition or erosion was identified by the Troels-Smith classification. Cores SIC2 and SIC3 were selected for further laboratory analyses as they had the clearest stratigraphic indication of potential storm surge evidence.

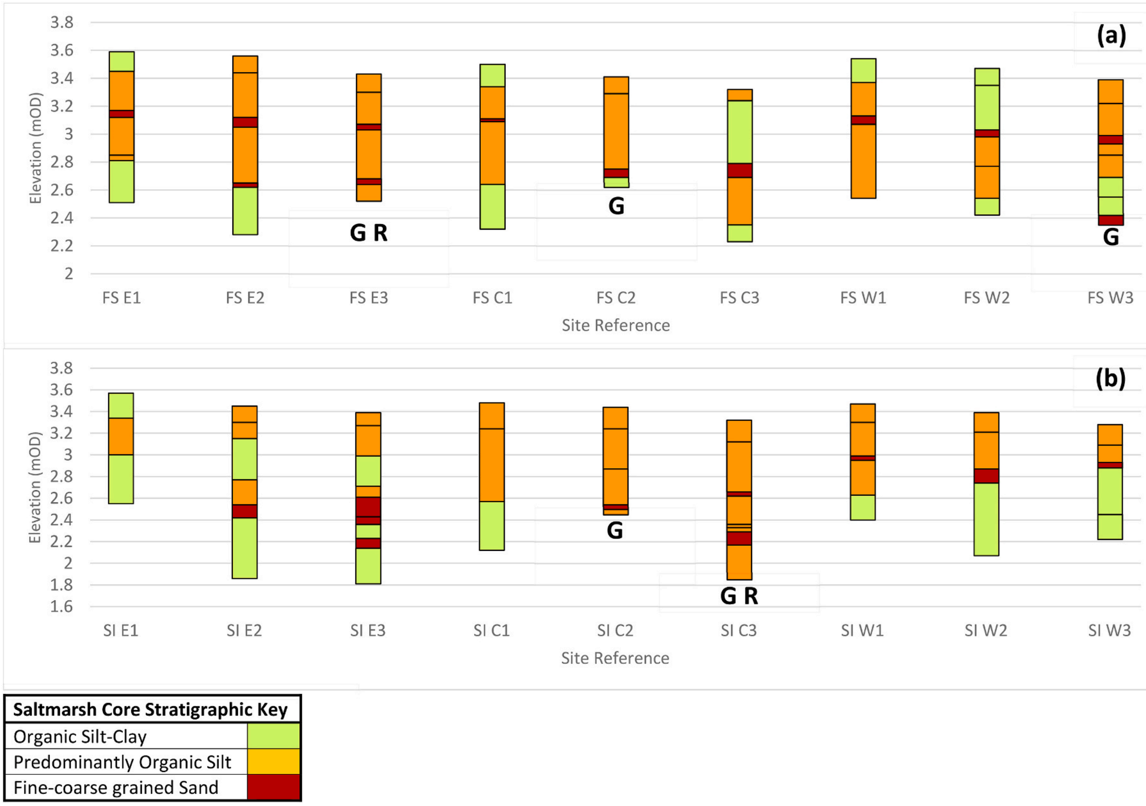

Fig. 2. Stratigraphy for the (a) Ferryside and (b) St. Ishmael sites. G = Geochemical analyses undertaken. G R = Geochemical and radionuclide analyses undertaken.

3.1.2. Geochemical data

The geochemical analyses were undertaken on five cores. The relative abundance of the select geochemical indicator elements against Ti and Rb throughout the cores and within the fine-coarse grained sand deposits was the main focus. In the five cores, the fine-coarse grained sand deposits (red horizons in Fig. 2) had a mean Ca count 94.2% and 77.6% higher against Ti and Rb compared to the respective overall relative elemental abundance throughout the cores. The mean Sr was 60.2% (Ti) and 46.9% (Rb) higher, whilst the increase in Ba was lesser increasing by 8.6% (Ti) and 1.9% (Rb). In the abrupt sand deposits, the mean K was 12.3% and 5.8% higher against Ti and Rb. The mean Si was 54.5% (Fe) and 42.3% (Rb) higher in the sandy deposits. For the fluvial (Ti) and offshore marine (Zr) indicators, Ti was 4.2% (Rb) lower whilst Zr was 5.2% (Rb) greater in sandy deposits. The analysis did not clearly indicate the presence of any other potential storm surge deposits or erosion.

Fig. 3 gives a wider perspective of the geochemical variability exhibiting the abundance of the indicator elements against depth in the cores selected for radionuclide analyses. For comparison, geochemistry is normalised (natural log (ln)) against Rb.

3.1.3. Particle size analysis

The three Ferryside cores showed greater particle size variability in comparison with the two St. Ishmael cores. The particle size increases corresponded with the sandy horizons identified in the Troels-Smith (1955) observations ((Fig. 3 (i-ii) (a and b)). Mean D50 values for abrupt sandy deposits are classified as medium sand and ranged from 263 μm (SIC2 2.50–2.54 mOD) to 331 μm (FSC2 2.67–2.75 mOD). D10 and D90 values highlighted the wide distribution of particle size within the sandy deposits as mean D10 values ranged from 28 μm to 41 μm (mean of averages = 34.6 μm). The mean D90 range from 469 μm to 632 μm (mean of averages = 544 μm) indicated the abundance of coarse sand (>500 μm). Fig. 3((b)(i-ii)) illustrates the abrupt increases in particle size (D10, D50 and D90) in dated cores. There were no abrupt increases in particle size that could have been indicative of deposition in smaller storm surge events.

3.1.4. Principal Component Analysis

The geochemical principal analyses highlighted that Sr, Ca and Si relative abundances were the most prominent elements distinguishing the abrupt, sandy deposits from the surrounding silt strata. Throughout the five cores particle size was consistently closer to the mean variance values for the sandy deposits than the values for all elements against Ti and Rb. An exception to the trend of particle size being the most prominent distinguishing overall factor for sandy deposits is found in FSW3 against Ti where Sr, Ca and Si have closer mean variance values.

3.1.5. Radionuclide dating

Core FSE3: The ^{210}Pb activity in FSE3 exhibited an upcore increase from the basal value of 0.022 Bq g^{-1} (±0.0076) at 2.50 mOD. Activity gradually increased up core with the exception of the increase to 0.034 Bq g^{-1} at 2.58 mOD which had the largest uncertainty of 0.0091 Bq g^{-1}. Activity markedly increased at 3.34 mOD to 0.060 Bq g^{-1} (±0.0033) reaching a maximum of 0.065 (±0.0045) at 3.42 mOD (see Fig. 4(i)(b)). As ^{137}Cs dating returned more accurate chronological markers, ^{210}Pb was only used to calculate sediment accretion and age below 2.78 mOD. From 2.51 to 2.78 mOD the ^{210}Pb CRS model (age-depth linear trend R^2 = 0.87) returned a SAR of 1.04 cm/yr.

Key markers in the FSE3 ^{137}Cs chronology enabled dating markers to be identified. Study of the ^{137}Cs profile indicated that the variations correspond to the marine radioactivity discharge patterns from the Sellafield Reprocessing Plant with a maximal output between 1978-80 (Gray et al., 1995). Uncertainty for ^{137}Cs measurement was constant at 0.0003 Bq g^{-1} and a 2 year transport lag uncertainty to the Bristol Channel from the Sellafield Plant (Tsompanoglou et al., 2011; Swindles et al., 2018) was accounted for. The first detectable ^{137}Cs activity was at 2.78 mOD corresponding with the onset of atmospheric thermonuclear testing (1952–54) (Fig. 4(i)(c)). Rapid increases in activity to 0.0025 Bq

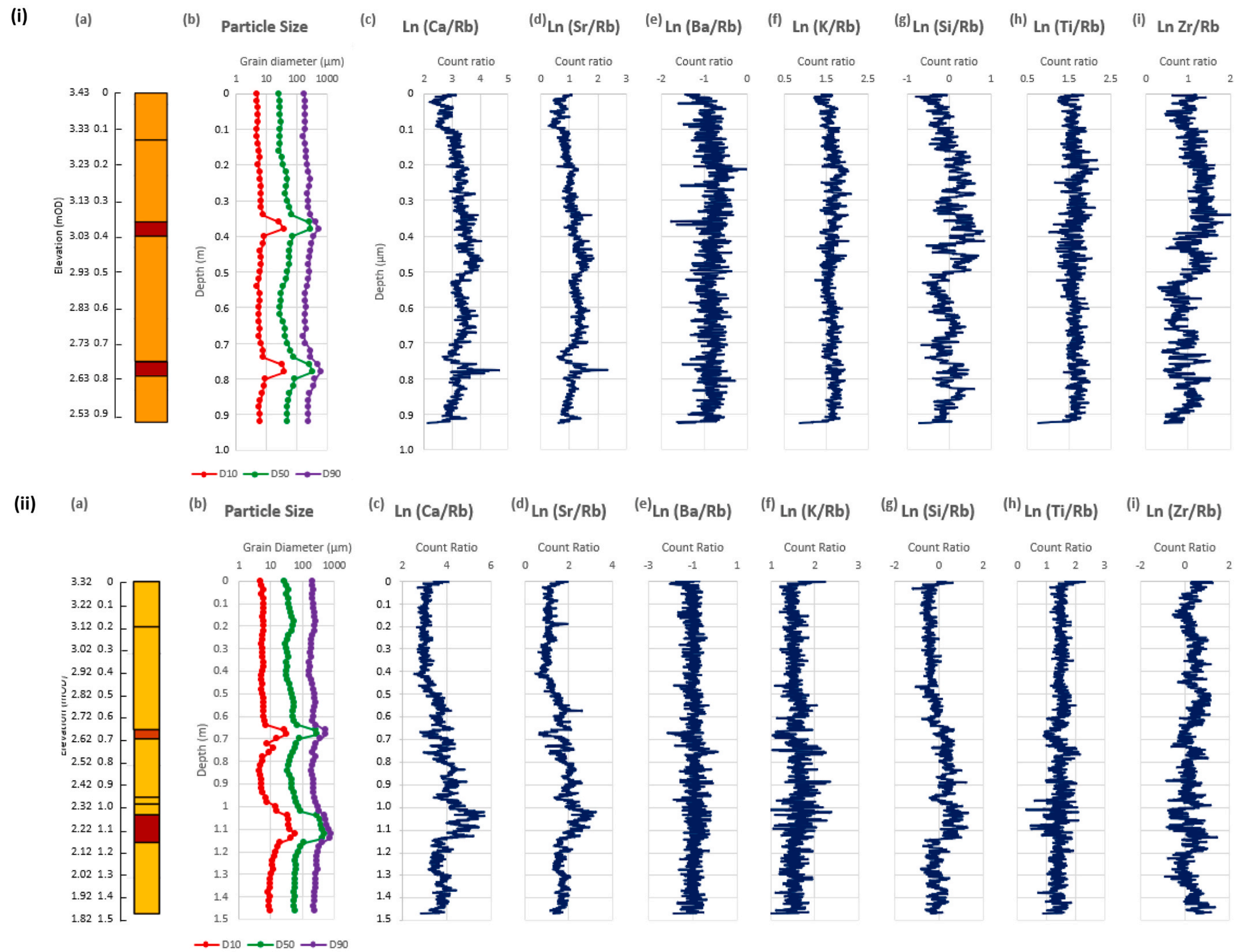

Fig. 3. Variability in (a) stratigraphy, (b) particle size and (c–i) indicator element abundance for cores (i) FSE3 and (ii) SIC3. The natural log of the elemental abundance relative to the conservative element Rb is shown for comparison.

g^{-1} at 2.86 mOD corresponded with the nuclear fallout maximum (1963). From 2.78 to 3.42 mOD similar ^{137}Cs SARs of 0.99, 1.02 and 0.96 cm/yr were produced for 0, +2a and -2a transport uncertainity respectively assuming the 3.03–3.07 mOD deposit was a discrete event. The combined ^{137}Cs and ^{210}Pb CRS models dated the sandy deposits at 2.64–2.68 mOD and 3.03–3.07 mOD as March 1949 (69.8 + 10.2–10.7 a from Feb 2019) and March 1984 (34.8 + 3.2–3.3 a from Feb 2019) respectively.

Core SIC3: This contained no detectable ^{137}Cs (later discussed) and therefore only ^{210}Pb was used. Pb-210 increased gradually from a basal value of 0.031 Bq g^{-1} (±0.0027) at 1.87 mOD before a rapid decrease to a minimum of 0.015 Bq g^{-1} (±0.0029) at 1.99 mOD. The activity gradually increased upcore to 3.03 mOD (see Fig. 4(ii)(b)). The ^{210}Pb CRS model (age linear trend $R^2 = 0.78$) for SIC3 returned a SAR of 1.43 cm/yr for the core. The base of SIC3 was the oldest sediment recorded dated January 1929 (90.1 ± 7.7 a) The sandy deposits at 2.17–2.29 mOD and 2.62–2.66 mOD were dated as March 1950 (68.8 ± 9.3 a) and April 1973 (45.7 ± 4.8 a).

3.2. Tidal gauge data

The tidal gauge analyses examined the greatest (top 1%) storm surges recorded at Newlyn (January 1915–June 1961) and Milford Haven (July 1961–December 2020). At Newlyn the greatest recorded elevation of 5.72 m AD was recorded on October 17, 1959 with a storm surge of 0.42 m. The greatest surge of 0.95 m occurred on November 12, 1915 (4.64 m AD). The greatest surge within the age range for both deposits FS E3 2.64–2.68 mOD and SI C3 2.17–2.29 mOD was 0.79 m on November 29, 1954 (5.44 m AD) (see Fig. 5).

At Milford Haven the greatest recorded elevation of 7.72 m AD was recorded on October 22, 1961 corresponding with a 0.89 m surge. The greatest storm surges of 1.49 m and 1.26 m were recorded on February 12, 2014 (4.16 m AD) and January 11, 1962 (2.39 m AD). Fig. 5 exhibits the tidal gauge data for storm surge height for classified high magnitude storms within each deposit date range. The greatest surge within the age range for the FS E3 3.03–3.07 mOD deposit was 0.92 m on December 13, 1981 (3.61 m AD). The greatest surge within the age range for the SI C3 2.62–2.66 mOD deposit was 1.18 m on January 12, 1974 (2.46 m AD).

3.3. Meteorological data

A meteorological assessment of all reported storms at Pembroke returned 1094 storms between 1861 and 2020. The greatest magnitude storm recorded as Beaufort Force 11 occurred during the storm of 11–17/11/1929. The annual storm frequency ranged between 18-0, with 1931 and 1938 being the stormiest years. Fig. 6 exhibits the

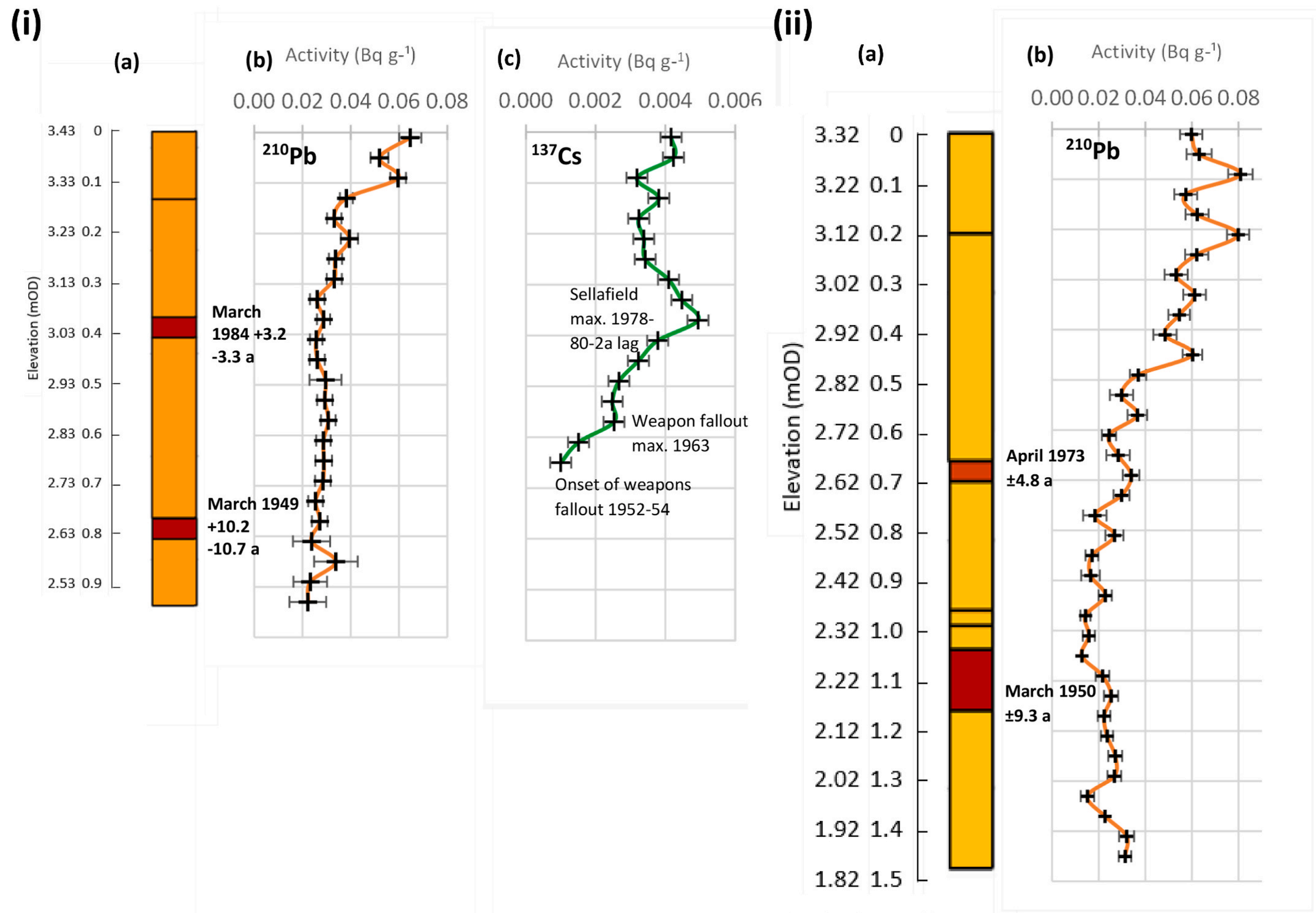

Fig. 4. (i-ii). Radionuclide chronology of (i) FSE3 and (ii) SIC3. Exhibited is (a) stratigraphy, (b) ^{210}Pb activity and (c) ^{137}Cs activity is exhibited. Decimalised ages in brackets are given before January 2019 and uncertainty is indicated.

meteorological data for wind magnitude for storms which correspond with the top 1% of storm surges. The strongest within the date range of the deposits FS E3 2.64–2.68 mOD and SI C3 2.17–2.29 mOD was Force 10 which occurred during the storm of 11–14/02/1950. For the deposit FS E3 3.03–3.07 mOD two Force 10 storms occurred during the storm of 13–15/12/1981 and 16–18/10/1982. For the deposit SI C3 2.62–2.66 mOD the strongest storms registered Force 9 during the storms of 5–16/11/1974 and 24–28/12/1977.

Fig. 7 shows the refined meteorological data for storms within the deposit radionuclide date ranges which were most likely to have produced sedimentological evidence in the Three Rivers Estuarine Complex (see section 2.6). South-west and Force 7 is the most common direction and magnitude combination. The strongest storms registering Force 10 were recorded from the WNW, WSW and SSW.

3.3.1. Storm correspondence

The storm events within the age uncertainty range for the four abrupt, sandy deposits in the cores SIC3 and FSE3 were identified using meteorological, tidal surge characteristics. The events considered were classified in the top 1% of storm surges (observed-predicted tidal height) at either the Newlyn or Milford tidal gauges and sorted via overall observed height (see 3.5 for rationale).

3.3.2. Core FSE3

For the 2.64–2.68 mOD deposit ^{210}Pb dating produced an age uncertainty of 21.0 yrs (1.d.p - 1938.5–1959.5) including 34 storms (Fig. 8(a)). The storms on 7–13/08/1948, 23–24/03/1955 and 4–5/11/1951 had the greatest overall observed surge heights of 5.2, 5.11 and 4.69 (m AD) at Newlyn. The greatest storm surges were recorded during the storms on 26–29/11/1954 (0.79 m), 18–19/12/1945 (0.69 m) as well as 2–5/02/1950 and 14–23/01/1939 (both 0.66 m). The greatest wind speed magnitude of force 10 was recorded during the 11–14/02/1950 storm. Force 9 was registered during six storms. The greatest storm surge events coincided with force 8 (0.79 m) and force 9 events (0.66–0.69 m).

For the 3.03–3.07 mOD deposit ^{137}Cs dating produced an uncertainty of 6.5a (1981.0–1987.5) including 3 events. The 24–30/03/1986 storm had the greatest overall observed surge height of 6.86 m AD coinciding with a surge of 0.77 m at Milford and a force 7 from the South-West. The 13–15/12/1981 storm resulted in a 4.83 m AD observed elevation and the largest surge of 0.91 m during a force 10 from the West-north-west.

3.3.3. Core SIC3

The ^{210}Pb deposit between 2.17 and 2.29 mOD produced an age uncertainty of 18.6 a (1941.0–1959.6) within which time 32 storms occurred (Fig. 8(b)). The storms of: 7–10/08/1948, 23–24/03/1955 and 4–5/11/1951 had the greatest overall observed surge heights of 5.2, 5.11 and 4.69 (m AD) at Newlyn. The greatest storm surge was recorded during the 26–29/11/1954 storm (0.79 m). The greatest storm wind speed magnitude was recorded during the storm of 11–14/02/1950 when a force 10 was registered at Pembroke once and a force 9 was registered six times. A wind direction between west and south was observed on 30/34 occasions.

The 2.62–2.66 mOD deposit ^{210}Pb dating produced an uncertainty of 9.6 yrs (1968.5–1978.1) within which period 4 storms occurred. The

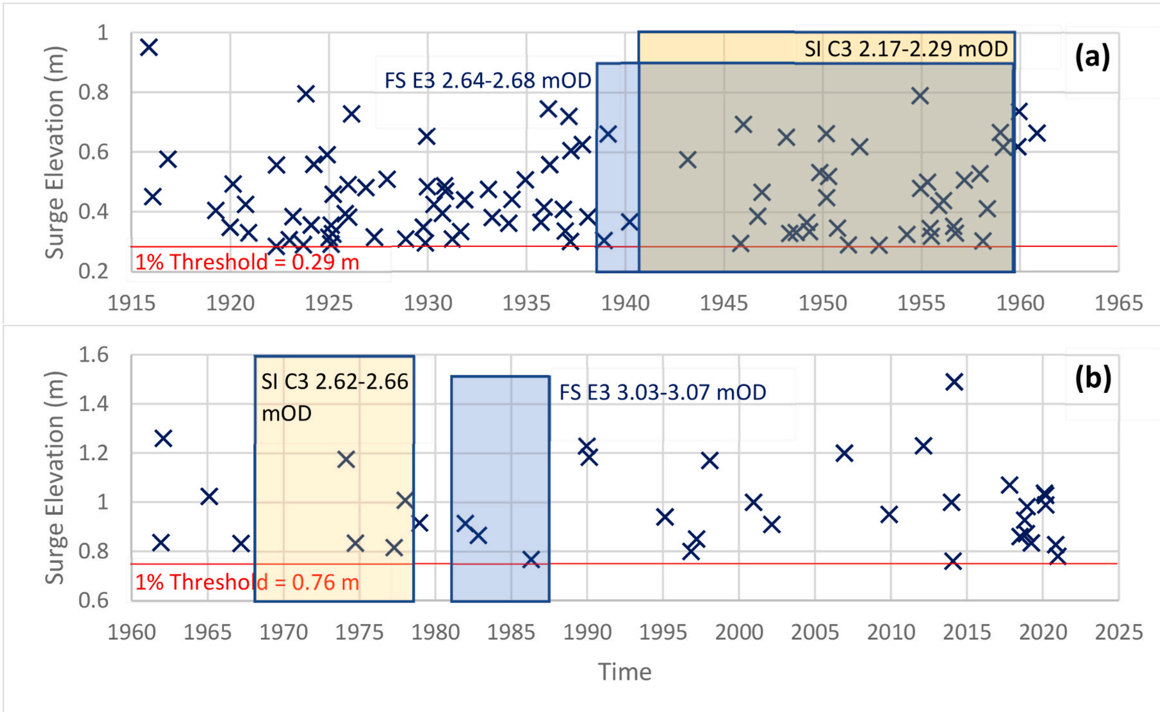

Fig. 5. Top 1% storm surges recorded at Newlyn (a) and Milford Haven (b). Yellow and blue zones respectively represent the radionuclide age ranges for the deposits in SI C3 and FS E3. (For interpretation of the references to colour in this figure legend, the reader is referred to the Web version of this article.)

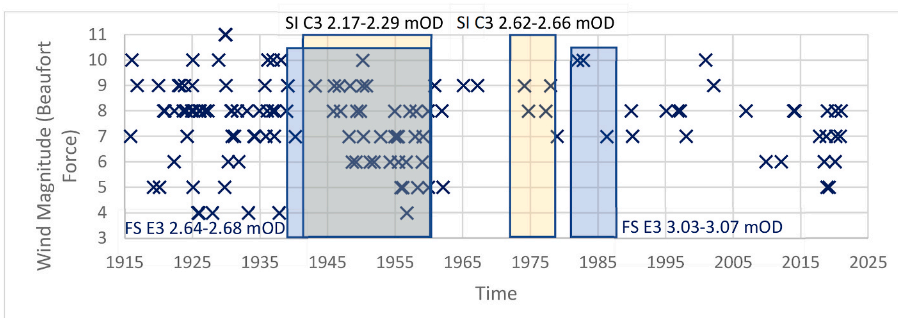

Fig. 6. Observed windspeed at Pembroke during top 1% storm surges at Newlyn and Milford Haven. Yellow and blue zones respectively represent the radionuclide age ranges for the deposits in SI C3 and FS E3. (For interpretation of the references to colour in this figure legend, the reader is referred to the Web version of this article.)

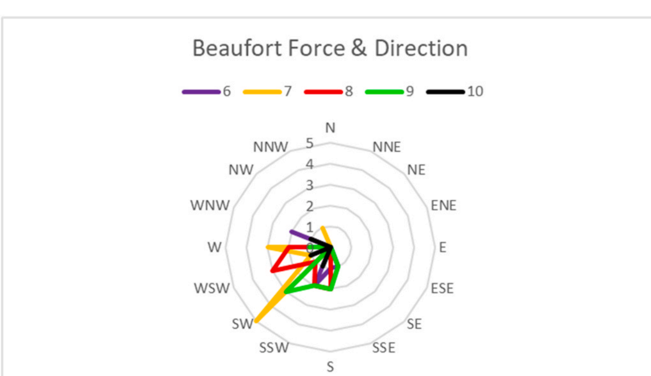

Fig. 7. Frequency of storms of a specific wind strength and direction within the radionuclide date range for all four deposits that conform to the criteria in 2.6.

storm on 13–15/03/1977 had the greatest overall observed surge height of 6.43 m AD which coincided with a 0.82 m surge at Milford. The greatest storm surge of 1.18 m occurred on 5–16/01/1974. The storms (24–28/12/1977 and 5–16/01/1974) in which the greatest storm surges were recorded, occurred during a force 9 storm. The wind direction varied from the south to west-south-west.

4. Interpretation and discussion

The meteorological, tidal gauge and sedimentological results exhibit archival correspondence between the data. Although a high number of storms correspond with each storm surge deposit, the detailed dated archival records, combined with a prior understanding of storm surge saltmarsh interaction (Leonardi et al., 2018; Garzon et al., 2019), enables the identification of the most plausible corresponding storms. The implications of these results for saltmarsh sustainability in the Three Rivers Estuarine Complex are subsequently discussed.

(a)

Date	Wind Speed Magnitude (Beaufort Force)	Direction wind	Storm Surge Height (m)	Observed Overall Height (m AOD)
24-30/03/1986	7	SW	0.769	6.859
16-18/10/1982	10	SSW	0.867	5.097
13-15/12/1981	10	WNW	0.915	4.83

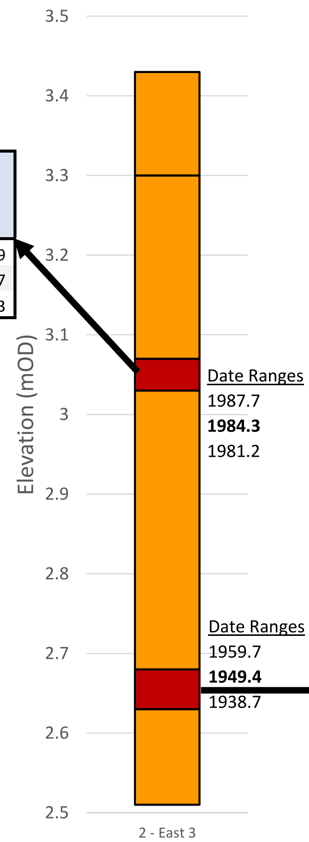

Date	Wind Speed Magnitude (Beaufort Force)	Wind Direction	Storm Surge Height (m)	Observed Overall Height (m AOD)
7-13/08/1948	7	NNW	0.3321	5.2
23-24/03/1955	7	SW	0.501	5.11
4-5/11/1951	6	SSE	0.619	4.69
26-29/11/1954	8	WSW	0.79	4.65
18-22/11/1959	7	SW	0.618	4.6
4-8/12/1954	7	W	0.48	4.43
18-20/03/1950	7	WSW	0.52	4.25
23-27/10/1945	8	SW	0.296	4.19
22-28/10/1952	7	W	0.29	3.99
14-23/01/1939	9	SW	0.662	3.83
30-4/03-04/1948	9	W	0.329	3.81
18-19/12/1945	9	SW	0.6939	3.6
9-10/10/1956	5	SSW	0.439	3.59
24-25/11/1946	8	S	0.4669	3.44
30-31/01/1943	9	SW	0.576	3.41
5-11/08/1958	8	W	0.304	3.39
11-14/02/1950	10	WSW	0.449	3.26
15-19/09/1950	9	S	0.3469	3.17
2-5/02/1950	9	SSW	0.663	3.11
6-8/08/1955	6	SSW	0.32	2.92
8-9/02/1949	6	WNW	0.366	2.77
31-5/01-02/1957	8	SSW	0.508	2.75
4-6/04/1949	8	WSW	0.335	2.74
19-23/12/1958	6	SSW	0.667	2.6
25-2/01/1948	7	SW	0.651	2.54
25-29/11/1938	8	W	0.3059	2.44
1-2/11/1955	5	W	0.423	2.25
3-4/04/1958	5	SW	0.412	2.23
28-4/08-09/1946	9	SSE	0.387	2.1
3-9/03/1954	6	S	0.326	1.46
4-5/09/1956	4	SSW	0.33	1.46
29-30/07/1956	6	WNW	0.353	1.43
8-11/12/1957	7	SW	0.529	1.29
22-27/02/1940	7	W	0.368	0.97
25-26/10/1949	8	SSW	0.533	0.96

Fig. 8(a). Correspondence between sedimentological, tidal gauge and meteorological data for core FSE3. Deposit radionuclide age ranges are displayed against the deposit.

4.1. Sedimentological evidence and archival correspondence

4.1.1. Sedimentological evidence and deposit origin

The stratigraphic analyses of the sampled cores exhibited abrupt sandy deposits measuring between 0.03 and 0.12 m. The PSAs (4.1.3) indicated that all sandy deposits were classified as medium-sand with D50 values ranging from 263 μm (SIC2 2.50–2.54 mOD) to 331 μm (FSC2 2.67–2.75 mOD). The D10 (mean of averages (moa) = 34.6 μm) and D90 (moa = 544 μm) range exhibited poor sorting. Poorly sorted sandy deposits several centimetres deep were initially indicative of plausible offshore marine surge deposition (Williams, 2010; Chaumillon et al., 2017; Leonardi et al., 2018).

The geochemical evidence (3.1.2) indicated a high relative abundance of Ca and Sr which suggests an offshore origin for the sandy deposits, most likely sourced from the sand dominated seabed of Carmarthen Bay (Cooper and McLaren, 2007; Liu et al., 2014). Mean Zr relative abundance was 5.2% (Rb) greater in the sandy deposits, whilst Ti was 4.2% lower (Rb) in deposits than the core average. This refutes aeolian and fluvial hypotheses (Tsompanoglou et al., 2011; Goslin and Clemmensen, 2017). The mean increases in K and Si support the PSA suggesting deposition during a high energy surge (see Section 3.1.3) (Williams et al., 2011; Chague-Goff et al., 2016). PCAs indicate that particle size was the most prominent distinguishing factor for abrupt sandy deposits whilst Sr, Ca and Si were the most prominent distinguishing elements followed by Ba, Br, Ti and K against Ti (excluding indicator Ti) and Rb (Section 3.1.4).

The geology of the Tywi catchment contains a channel that flows through an alluvial valley between Ordovician Shale beds (Geological Survey, 2021). Although Carmarthen Bay has formed upon a glacial sand and gravel deposit, the Tywi is largely defended there and follows a highly sinuous course on approach (Ahmed and Hodge, 2017) reducing the transportation of glacial sediment downstream during fluvial floods. Red marl and sandstone as well as micaceous sandstone respectively comprise the bedrock of the elevated areas surrounding the Tywi and Gwendraeth estuaries. However, a combination of surrounding glacial boulder clay and coastal defence means neither substantially erodes the sandstone bedrock (Geological Survey, 2021). Considering both the sedimentological evidence of this study and catchment geology, it is unlikely the deposits originate from a fluvial flood event. Alternatively, Carmarthen Bay is underlain by Carboniferous and Devonian limestones and sandstones beneath the sand-dominated seafloor (Cooper and McLaren, 2007; Countryside Council for Wales, 2009). Given the geological predominance of sand on the seafloor, particularly from the south-south-east to west of the mouth of the estuarine complex, it is therefore most likely the deposits result from a high energy inundation event of offshore marine origin.

Although theories of tsunami deposits on the Bristol Channel coastline concerning the Great Flood of 1607 have been suggested (Bryant and Haslett, 2002), recent research suggests storm surges and meteotsunamis are the most likely sources (e.g. Horsburgh and Horritt., 2006; Westlake, 2019). When research concerning the hydrological and geomorphological storm impacts on the Three Rivers Estuarine Complex

(b)

Date	Wind Speed (Beaufort Force)	Wind Direction	Storm Surge Height (m)	Observed Overall Height (m AD)
13-15/03/1977	8	S	0.817	6.427
7-8/09/1974	8	WSW	0.835	3.535
24-28/12/1977	9	SSW	1.01	2.8
5-16/01/1974	9	S	1.177	2.457

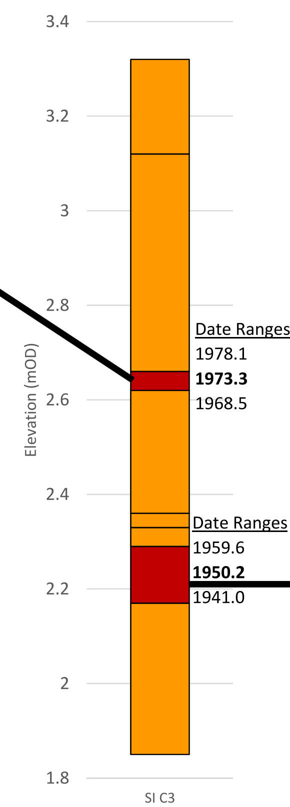

Date	Wind Speed Magnitude (Beaufort Force)	Direction wind	Storm Surge Height (m)	Observed Overall Height (m AOD)
7-10/08/1948	7	NNW	0.332	5.2
23-24/03/1955	7	SW	0.501	5.11
4-5/11/1951	6	SSE	0.619	4.69
26-29/11/1954	8	WSW	0.79	4.65
18-22/01/1959	7	SW	0.618	4.6
4-8/12/1954	7	W	0.48	4.43
18-20/3/1950	7	WSW	0.52	4.25
23-27/10/1945	8	SW	0.296	4.19
22-28/10/1952	7	W	0.29	3.99
30-4/04/1948	9	W	0.329	3.81
18-19/12/1945	9	SW	0.6939	3.6
9-10/01/1956	5	SSW	0.439	3.59
24-25/11/1946	8	S	0.4669	3.44
30-31/01/1943	9	SW	0.576	3.41
5-11/01/1958	8	W	0.304	3.39
11-14/02/1950	10	WSW	0.449	3.26
15-19/09/1950	9	S	0.3469	3.17
2-5/02/1950	9	SSW	0.663	3.11
6-8/06/1955	6	SSW	0.32	2.92
8-9/02/1949	6	WNW	0.366	2.77
31-5/02/1957	8	SSW	0.508	2.75
4-6/04/1949	8	WSW	0.335	2.74
17-18/05/1955	7	SSE	0.346	2.72
19-23/12/1958	6	SSW	0.667	2.6
25-2/01-02/1948	7	SW	0.651	2.54
1-2/11/1955	5	W	0.423	2.25
3-4/04/1958	5	SW	0.412	2.23
28-4/08-09/1946	9	SSE	0.387	2.1
3-9/03/1954	6	S	0.326	1.46
4-5/09/1956	4	SSW	0.33	1.46
29-30/07/1956	6	WNW	0.353	1.43
8-11/12/1957	7	SW	0.529	1.29
25-26/10/1949	8	SSW	0.533	0.96

Fig. 8(b). Correspondence between sedimentological, tidal gauge and meteorological data for the deposit between 2.17 and 2.29 mOD and 2.62–2.66 mOD in core SIC3. Deposit radionuclide age ranges are displayed against the deposit.

(Pye and Blott, 2009; Bennett et al., 2019) is considered with the sedimentological evidence, it is most plausible the abrupt sandy deposits were produced during high magnitude storm surge events.

4.1.2. Sedimentological and archival correspondence

The number of storms corresponding with the dated deposits varies depending on the age-dependent radionuclide used (section 4.4). Despite an initially high number of corresponding events (max 34), when storm surge dynamics and other regional research is considered the number of plausible corresponding events is reduced to 1–3 depending on the deposit.

The stratigraphical evidence (3.1.1) indicates little geomorphological change with the exception of the abrupt sandy surge deposits. This corroborates with previous research that suggests limited geomorphological change in the estuarine complex before 1938 (oldest deposit uncertainty) as the saltmarshes accreted uniformly relative to SLR (Bristow and Pile, 2003; Pye and Blott, 2009). A prolonged period of surge inundation would theoretically allow the transportation and deposition of sand to the middle marsh at high tide (Hawkes and Horton, 2012; Garzon et al., 2019). Coarse offshore marine sediment could not reach such elevations at lower tides (regardless of storm surge elevation) due to the high interception rate of the dominant *Spartina anglica* (Rupprecht et al., 2017), and shortened inundation and depositional period (Williams and Flanagan, 2009; Leonardi et al., 2018). Therefore, the evidence suggests only surges coinciding with large overall tidal elevations could be depositional events.

According to the radionuclide dates, FSE3 deposits between 2.64 and 2.68 mOD and 3.03–3.07 mOD exhibit temporal correspondence with 34 and three events respectively. While the event of 7–13/08/1948 corresponds with the largest observed tidal height of 5.20 m AD at Newlyn, this occurred with a comparatively small surge height of 0.33 m and a recorded wind direction NNW at Pembroke. As Ferryside is near the head of the Tywi estuary (Fig. 1(ii)) and the predominant storm wave and wind direction in Carmarthen Bay for storms with a ≥1 year return period of 225° (SW) (Bennett et al., 2019), this is unlikely to be the deposit source. Although the 4–5/11/1951 storm with the third highest observed surge height may have produced the deposit, location and bathymetry means SSE winds registering Force 6 are unlikely to have produced the deposit when storm wave propagation is considered. The large decrease in the observed elevation after the 4–5/11/1954 storm of 0.22 m rules out other events leaving the 23–24/03/1955 and 26–29/11/1954 storms.

The two events have wind directions that would likely permit storm wave propagation and offshore sediment transportation up the River Tywi. Whilst the event of 23–24/03/1955 corresponds with the second highest overall elevation at Newlyn of 5.11 m AD, it only ranks as the eighth greatest storm surge in the 21.0 year uncertainty period at 0.50 m. The event of the 26–29/11/1954 had an elevation of 4.65 m AD and a surge of 0.79 m which was the greatest in the period (mean = 0.47 m). The meteorological information indicates it corresponded with a Force 8 whereas the 23–24/03/1955 event occurred during a Force 7. Given the rarity of deposits and the very high levels of wave energy needed to transport and deposit 0.04 m of coarse material on the Ferryside saltmarshes (Pye and Blott, 2009; Horton et al., 2009; Swindles et al., 2018), the evidence suggests the FSE3 2.64–2.68 mOD deposit most plausibly originates from the 26–29/11/1954 storm (see Table 2).

The ^{137}Cs dated deposit between 3.03 and 3.07 mOD in FSE3 had three corresponding storms. The meteorological characteristics of the two storms on 13–15/12/1981, 16–18/10/1982 were similar with a maximum wind strength magnitude of Force 10 from the WNW. The storm of 24–30/03/1986 corresponds with a lower storm strength of Force 7 from the SW. All would produce storm wave conditions in the Tywi estuary (Bennett et al., 2019).

The surge of 13–15/12/1981 was the largest at 0.92 m being just below the mean of the top 1% surges (0.99 m). The overall height of the 24–30/03/1986 storm of 6.86 m made it the sixth largest at Milford Haven (1961–2020) during a top 1% storm surge (mean = 4.35 m) while the 16–18/10/1982 storm elevation was 5.10 m. Although the observed overall elevation of the 13–15/12/1981 was the smallest, there is clear additional evidence that this event had a profound geomorphological impact in the Bristol Channel. The study by Croudace et al. (2012) was the first and only to identify the broad tidal and sub-tidal erosional impact of the December 1981 storm surge in the Severn Estuary. The study provided convincing geochemical, sedimentological and radiochronological evidence to show a substantial hiatus in the sedimentary record from cores collected east of Cardiff and the Newport Deep. Sub-tidal erosion linked to the 1981 storm was also identified in cores from Bridgwater Bay (currently unpublished work; pers. comm. Croudace). The temporal correspondence, Force 10 windspeed magnitude and the fact the event also produced major geochemical and sedimentological discontinuities in the region, renders the 13–15/12/1981 storm the most plausible source of the 3.03–3.07 mOD deposit.

The two deposits in core SIC3 exhibit a similar trend of correspondence with the deposits between 2.17 and 2.29 mOD and 2.62–2.66 mOD corresponding with 32 and four storms respectively. For the 2.17–2.29 mOD deposit the ^{210}Pb dating uncertainty range of 18.6 years (1941.0–1959.6) means the top four observed storm surges are the same as those which correspond with the 2.64–2.68 mOD deposit in FSE3. The fifth greatest surge occurred during the 18–22/01/1959 storm, with an overall observed elevation of 4.6 m AD in a Force 7 from the SW which would hypothetically produce a storm surge wave in the mouth of River Gwendraeth (see Fig. 1). However, the surge elevation was only 0.62 m. Therefore, it is most plausible that this deposit was from the 26–29/11/1954 storm (see Table 2).

The 2.62–2.66 mOD deposit had a^{210}Pb age uncertainty between 1968.5 and 1978.1. The four events all have suitable meteorological characteristics to produce storm surge waves at the mouth of the River Gwendraeth. Although the event of the 13–15/03/1977 has the smallest storm surge elevation (0.82 m) the observed overall elevations of the three other events were ≤0.81 m, the mean of all recorded events (4.35 m AD). In contrast, the 13–15/03/1977 storm was the tenth greatest observed elevation at Milford Haven. Therefore, when the evidence is considered with the conditions of saltmarsh storm surge deposition (Horton et al., 2009; Garzon et al., 2019), it is most plausible the storm of 13–15/03/1977 produced the 2.62–2.66 mOD deposit (see Table 2).

Table 2
Most plausible corresponding storm events for the four deposits in cores FSE3 and SIC3.

Core and Depth	Date	Wind Speed (Beaufort Force)	Wind Direction (Compass Bearing)	Storm Surge Height (m)	Observed Overall Height (m AD)
FSE3 3.03–3.07 mOD	13-15/12/1981	10	WNW	0.92	4.83
SIC3 2.62–2.66 mOD	13-15/03/1977	8	S	0.82	6.43
FSE3 2.64–2.68 mOD & SIC3 2.17–2.29 mOD	26-29/11/1954	8	WSW	0.79	4.65

4.2. Implications for saltmarsh sustainability

This research exhibits the potential of saltmarshes to preserve storm surge depositional evidence, however, the data shows this preservation is rare with just 3 events likely being preserved. While the data shows major storm surge deposition can contribute to sustaining saltmarsh elevation relative to sea level, storms have likely had a range of impacts on the saltmarshes of the Three Rivers Estuarine Complex. Plausible alternative impacts aside from major (>3 cm deposits) deposition include erosion, micro-deposition and the discrete deposition of very coarse sediment (granules and pebbles), while erosional events can also erode previous deposits (Horton et al., 2009; Tsompanoglou et al., 2011; Croudace et al., 2012; Leonardi et al., 2016). It is also highly plausible storms may have negligible sedimentological impacts if the meteorological, bathymetry and environmental conditions hinder surge wave propagation or are conducive to effective wave dissipation, preventing substantial erosion or deposition (Spencer et al., 2016; Rupprecht et al., 2017). The combined sedimentological and archival findings highlight there still remains uncertainty surrounding the regional impacts (or non-impacts) on the Three Rivers Estuarine Complex saltmarshes with the rare occurrence of major deposition. This raises important questions regarding the future sedimentological and geomorphological impacts of coastal storms on the saltmarsh environments.

According to the climatic and surge models (Lowe et al., 2018; Palmer et al., 2018), as well meteorological and tidal gauge research (Slingo et al., 2014; Wadey et al., 2014), the frequency of high magnitude storms and storm surges is increasing and projected to further increase from the UKCP 1981–2000 baseline. The anticipated SLR of 0.7 m by 2100 according to the most probable (current emissions) IPCC RCP 8.5 (SSP5 8.5) scenario and storm surge skew increase of 0.07 mm/yr (Palmer et al., 2018; Schwalm et al., 2020) is likely to increase the magnitude and frequency of storm surges in Carmarthen Bay. Given this high likelihood of increasing storminess, the variable findings on sedimentological storm impacts and the current sedimentological evidence, it is plausible that the Three Rivers Estuarine Complex saltmarshes will increasingly experience highly variable sedimentological change. This could have diverse geomorphological and ecological effects on the Three Rivers Estuarine Complex and determine to what extent the saltmarshes can sustain themselves relative to rising sea levels.

Whilst accretion has matched and, in some cases, exceeded SLR due to anthropogenic interference in areas of the Three Rivers Estuarine Complex (Bennett et al., 2020), whether this continues depends upon a range of climatological, hydrological and geomorphological factors. According to current research regional saltmarshes are predicted to recede and degrade as a result of SLR and climatic change in the Bristol Channel. Specifically, relative SLR in south-west Wales has a >80% probability of causing saltmarsh retreat and degradation under the RCP 8.5 (SSP5 8.5) scenario by 2060 (Horton et al., 2018; Schwalm et al., 2020). This is an issue at Ferryside and St. Ishmael at the Three Rivers Estuarine Complex as engineered coastal defences constrain the saltmarshes and the 50–100 year policy is to hold the line (Phillips et al., 2012). Therefore, although storm surge deposition currently contributes to sustaining saltmarsh elevation, if relative SLR exceeds accretion, a combination of increased hydroperiod and storm erosional activity may lead to saltmarsh degradation in anthropogenically constrained areas such as the Three Rivers Estuarine Complex (Bullimore, 2014). In these areas, saltmarshes cannot establish equilibrium as recession is prevented potentially catalysing environmental degradation through coastal squeeze and creek propagation (Hughes et al., 2009; Doody, 2013; Crosby et al., 2016).

Despite the regional modelled predictions (Horton et al., 2018) it is also plausible that increased surge frequency could augment saltmarsh accretion through storm deposition (Williams and Flanagan, 2009; Leonardi et al., 2018). Storm deposition of sediment ranging between 0.04 and 0.12 m thick could offer a great contribution to sustaining saltmarshes even if this occurred as irregularly as exhibited in this study. Given that since 4 kyr BP the best estimate for relative sea level rise in the Bristol channel is 0.76 mm/yr or 7.6 cm per 100 a (Shennan and Horton, 2002; Shennan et al., 2018) it is theoretically plausible that storm surge deposits could offer a major contribution to sustain regional saltmarshes, regardless of increased SLR (Pannozzo et al., 2021). While possible, as this multidisciplinary study has demonstrated, very specific tidal, meteorological and geomorphological conditions are required for notable storm surge accretion to occur (de Groot et al., 2011), so such events cannot be relied upon to sustain the saltmarshes. The balance between erosional and depositional events is also a key factor, determined by sediment supply as well as meteorological and environment dynamics which requires further regional research. The predicted saltmarsh vegetation recession resulting from relative SLR could further reduce deposition and preservation of deposits as reduced vegetation dampening makes storm accretion less plausible (Woodroffe and Long, 2009; Chaumillon et al., 2017; Horton et al., 2018). This relationship is highly complex however, as storm surge deposition results in abrupt sediment geochemical and particle size change which would influence biological productivity (Capooci et al., 2019). Therefore changing storm surge deposition could itself contribute to biological changes effecting saltmarsh erodibility and sustainability. The predicted progressive changes in climate and weather trends until 2100 add another complex dimension as this could further influence saltmarsh biological productivity and influence the erosion-deposition balance (Zedler, 2010; Prahalad et al., 2012). This diverse combination of influencing factors render future saltmarsh sustainability uncertain.

Alternatively, it has been shown that saltmarshes in North-west Europe such as those in the Three Rivers Estuarine Complex have historically widely sustained themselves relative to sea level rise and the regional threat could be seen as overestimated (e.g. French, 2006; Kirwan et al., 2016). Instead it is more often that direct human interference influencing sediment supply, tidal range and limiting transgression that causes degradation (Kirwan and Megonigal, 2013; Vinent et al., 2019). As Carmarthen Bay is a protected region it could therefore be argued that based on past evidence there is no reason why it should degrade, as a combination of progressive sedimentation and sporadic storm surge has previously maintained saltmarsh elevation. However, the substantial predicted increases in atmospheric storminess, sea level rise and associated saltmarsh degradation (Horton et al., 2018; Lowe et al., 2018) are unlike any seen from January 1929–February 2019. Therefore, given the future climate and environmental response uncertainties combined with the uncertainty surrounding storm sedimentological saltmarsh impacts, major changes in the saltmarsh sustainability up to 2100 cannot be ruled out.

Although past evidence indicates that a combination of organic sediment accumulation and sporadic storm surge deposition has enabled the saltmarshes to sustain themselves relative to sea level rise, future regional predictions give cause for concern as high magnitude storms become more frequent. Predicted increases in storminess, sea level rise and saltmarsh degradation, could pose new threats to the regional saltmarshes. Given the uncertainties surrounding sedimentological storm saltmarsh impacts and the increasing frequency of high magnitude storms similar to Storm Eustice in 2022, it is important that storms are further investigated in the Three Rivers Estuarine Complex. This is essential to monitor the sustainability of a valuable blue carbon store that provides important saltmarsh ecosystem services to the natural and human populations (Craft et al., 2009; Pendleton et al., 2012; Gilby et al., 2021).

5. Summary

This study uses meteorological, tidal gauge and sedimentological evidence to appraise the impact of coastal storms in the saltmarshes of the Three Rivers Estuarine Complex, Carmarthen Bay. The sedimentological research identifies that major storm surge deposition likely occurred between 1929 and 2019. The combined evidence indicates that the storms of the 26–29/11/1954 (two deposits), 13–15/03/1977 and 13–15/12/1981 are the most plausible storms recorded in the sediments. No clear sedimentological evidence of storm erosion or alternative types of deposition was identified. The tidal and meteorological records exhibit the comparatively rare occurrence of major depositional events compared to the number of storms in the tidal and meteorological records. Therefore, considerable uncertainty still surrounds the sedimentological impacts of storms in the estuarine complex. The diverse range of plausible saltmarsh sedimentological impacts merit further investigation given the increasing regional storm prevalence. It could be argued the historical evidence highlights that organic accumulation and sporadic storm surge deposition could enable the saltmarshes to maintain elevation relative to rising sea levels. However, the predicted increases in regional relative sea level and high magnitude storm frequency coupled with the >80% probability of regional saltmarsh retreat (Horton et al., 2018; Lowe et al., 2018; Palmer et al., 2018) give cause for concern in the 21st century. This is heightened by the limited ability of the saltmarshes to transgress and maintain equilibrium due to manmade coastal defences and the current 50–100 year coastal defence policy in the estuarine complex. When the sedimentological uncertainties and future threats are considered, this study suggests more research is required to explore the uncertain sedimentological impacts of storms in the region. This could contribute to sustaining the vulnerable coastal saltmarsh environments and the important ecosystem services they provide.

CRediT authorship contribution statement

Alexander Jardine: Writing – review & editing, Writing – original draft, Visualization, Methodology, Investigation, Formal analysis, Data curation, Conceptualization. **Katherine Selby:** Writing – review & editing, Validation, Supervision, Methodology, Funding acquisition, Conceptualization. **Ian W. Croudace:** Writing – review & editing, Validation, Software, Resources, Formal analysis. **David Higgins:** Writing – review & editing, Validation, Supervision.

Declaration of competing interest

The authors declare that they have no known competing financial interests or personal relationships that could have appeared to influence the work reported in this paper.

Acknowledgement

This research was funded by a White Rose College of the Arts and Humanities (Arts and Humanities Research Council) Network grant (PI Dr Katherine Selby). Thanks are due to GAU-Radioanalytical (Southampton) who undertook the radionuclide dating. Independent referees and reviewers are also thanked for their contributions.

References

Ahmed, J., Hodge, M., 2017, April. Morphological change on the River Towy, Wales assessed using aerial photogrammetry. In: EGU General Assembly Conference *Abstracts*, p. 1291.

Andersen, T.J., 2017. Some practical considerations regarding the application of ^{210}Pb and ^{137}Cs dating to estuarine sediments. In: Weckström, K., Saunders, K.M., Gell, P. A., Skilbeck, C.G. (Eds.), Applications of Paleoenvironmental Techniques in Estuarine Studies. Springer, Dordrecht, pp. 121–140.

Appleby, P.G., 2002. Chronostratigraphic techniques in recent sediments. In: Tracking Environmental Change Using Lake Sediments. Springer, Dordrecht, pp. 171–203.

GALE, 2021. GALE primary sources. Available: https://www.gale.com/intl/primary-sources. Last accessed 28th Septmeber 2021.
Baskaran, M., Nix, J., Kuyper, C., Karunakara, N., 2014. Problems with the dating of sediment core using excess ^{210}Pb in a freshwater system impacted by large scale watershed changes. J. Environ. Radioact. 138, 355–363.
Bennett, W.G., van Veelen, T.J., Fairchild, T.P., Griffin, J.N., Karunarathna, H., 2019. Computational modelling of the impact of salt marsh management interventions on coastal flooding. In: Proceedings for the 4th IMA International Conference on Flood Risk. Swansea, United Kingdom, pp. 2–9.
Bennett, W.G., van Veelen, T.J., Fairchild, T.P., Griffin, J.N., Karunarathna, H., 2020. Computational modelling of the impacts of saltmarsh management interventions on hydrodynamics of a small macro-tidal estuary. J. Mar. Sci. Eng. 8 (5), 373.
Blott, S.J., Pye, K., 2001. GRADISTAT: a grain size distribution and statistics package for the analysis of unconsolidated sediments. Earth Surf. Process. Landforms 26 (11), 1237–1248.
Bristow, C., Pile, J., 2003. South Wales Estuaries Camarthen Bay: Evolution of Estuarine Morphology and Consequences for SAC Management. Countryside Council for Wales, Bangor, UK, pp. 3–9.
British Oceanographic Data Centre, 2021. Search the data. Available: https://www.bodc.ac.uk/data/hosted_data_systems/sea_level/uk_tide_gauge_network/. (Accessed 4 September 2021).
Bryant, E.A., Haslett, S.K., 2002. Was the AD 1607 coastal flooding event in the Severn Estuary and Bristol Channel (UK) due to a tsunami? Archaeol. Severn Estuary 13, 163–167.
Bullimore, B., 2014. Problems and pressures, management and measures in a site of marine conservation importance: Carmarthen Bay and Estuaries. Estuar. Coast Shelf Sci. 150, 288–298.
Bunzel, D., Milker, Y., Müller-Navarra, K., Arz, H.W., Schmiedl, G., 2021. North Sea salt-marsh archives trace past storminess and climate variability. Global Planet. Change 198, 103403, 1-11.
Burden, A., Smeaton, C., Angus, S., Garbutt, A., Jones, L., Lewis, H., Rees, S., 2020. Impacts of climate change on coastal habitats, relevant to the coastal and marine environment around the UK. MCCIP Science Review 2020, 228–255.
Capooci, M., Barba, J., Seyfferth, A.L., Vargas, R., 2019. Experimental influence of storm-surge salinity on soil greenhouse gas emissions from a tidal salt marsh. Sci. Total Environ. 686, 1164–1172.
Carmarthenshire County Council, 2019. Part 2-policy unit level summaries. Flood Risk Management Plan 1 (2), 14–16.
Chague-Goff, C., Chan, J.C.H., Goff, J., Gadd, P., 2016. Late Holocene record of environmental changes, cyclones and tsunamis in a coastal lake, Mangaia, Cook Islands. Isl. Arc 25 (5), 333–349.
Chaumillon, E., Bertin, X., Fortunato, A.B., Bajo, M., Schneider, J.L., Dezileau, L., Walsh, J.P., Michelot, A., Chauveau, E., Créach, A., Hénaff, A., 2017. Storm-induced marine flooding: lessons from a multidisciplinary approach. Earth Sci. Rev. 165, 151–184.
Chen, D., Rojas, M., Samset, B.H., Cobb, K., Diongue Niang, A., Edwards, P., Emori, S., Faria, S.H., Hawkins, E., Hope, P., Huybrechts, P., Meinshausen, M., Mustafa, S.K., Plattner, G.-K., Tréguier, A.-M., 2021. Framing, context, and methods. In: Masson-Delmotte, V., Zhai, P., Pirani, A., Connors, S.L., Péan, C., Berger, S., Caud, N., Chen, Y., Goldfarb, L., Gomis, M.I., Huang, M., Leitzell, K., Lonnoy, E., Matthews, J. B.R., Maycock, T.K., Waterfield, T., Yelekçi, O., Yu, R., Zhou, B. (Eds.), Climate Change 2021: the Physical Science Basis. Contribution Of Working Group I to the Sixth Assessment Report Of the Intergovernmental Panel On Climate Change. Cambridge University Press, pp. 1–105.
Cooper, B., McLaren, P., 2007. An application of sediment trend analysis to Carmarthen Bay, Bristol Channel. Geol. Soc. Lond. Special Publ. 274 (1), 117–125.
Countryside Council for Wales, 2009. Carmarthen bay and estuaries/Bae Caerfyrddin ac aberoedd European marine site. Available: https://naturalresources.wales/media/673515/Carmarthen%20Bay%20R33%20Advice%20February%202009.pdf. (Accessed 8 July 2021).
Craft, C., Clough, J., Ehman, J., Joye, S., Park, R., Pennings, S., Guo, H., Machmuller, M., 2009. Forecasting the effects of accelerated sea-level rise on tidal marsh ecosystem services. Front. Ecol. Environ. 7 (2), 73–78.
Crosby, S.C., Sax, D.F., Palmer, M.E., Booth, H.S., Deegan, L.A., Bertness, M.D., Leslie, H. M., 2016. Salt marsh persistence is threatened by predicted sea-level rise. Estuar. Coast Shelf Sci. 181, 93–99.
Croudace, I.W., Rothwell, R.G. (Eds.), 2015. Micro-XRF Studies of Sediment Cores: Applications of a Non-destructive Tool for the Environmental Sciences, 17. Springer, Dordrecht, p. 668.
Croudace, I.W., Rindby, A., Rothwell, R.G., 2006. ITRAX: description and evaluation of a new sediment core scanner. In: Rothwell, R.G. (Ed.), New Techniques in Sediment Core Analysis. Geol. Soc. Spec. Publ., 267, pp. 51–63.
Croudace, I.W., Warwick, P.E., Morris, J.E., 2012. Evidence for the preservation of technogenic tritiated organic compounds in an estuarine sedimentary environment. Environ. Sci. Technol. 46 (11), 5704–5712.
Dawson, D., Shaw, J., Gehrels, W.R., 2016. Sea-level rise impacts on transport infrastructure: the notorious case of the coastal railway line at Dawlish, England. J. Transport Geogr. 51, 97–109.
de Groot, A.V., Veeneklaas, R.M., Bakker, J.P., 2011. Sand in the salt marsh: contribution of high-energy conditions to salt-marsh accretion. Mar. Geol. 282 (3–4), 240–254.
Dezileau, L., Sabatier, P., Blanchemanche, P., Joly, B., Swingedouw, D., Cassou, C., Castaings, J., Martinez, P., Von Grafenstein, U., 2011. Intense storm activity during the little Ice age on the French Mediterranean coast. Palaeogeogr. Palaeoclimatol. Palaeoecol. 299 (1–2), 289–297.
Doody, J.P., 2013. Coastal squeeze and managed realignment in southeast England, does it tell us anything about the future? Ocean Coast Manag. 79, 34–41.
Font, E., Veiga-Pires, C., Pozo, M., Nave, S., Costas, S., Muñoz, F.R., Abad, M., Simões, N., Duarte, S., Rodríguez-Vidal, J., 2013. Benchmarks and sediment source (s) of the 1755 Lisbon tsunami deposit at Boca do Rio Estuary. Mar. Geol. 343, 1–14.
French, J., 2006. Tidal marsh sedimentation and resilience to environmental change: exploratory modelling of tidal, sea-level and sediment supply forcing in predominantly allochthonous systems. Mar. Geol. 235 (1–4), 119–136.
Frew, C., 2014. Chapter 4. Coring Methods. Cook, SJ, Clarke, *LE, Nield, JM Geomorphological Techniques*, Online edition. British Society for Geomorphology, London, pp. 1–10.
Garzon, J.L., Maza, M., Ferreira, C.M., Lara, J.L., Losada, I.J., 2019. Wave attenuation by Spartina saltmarshes in the Chesapeake Bay under storm surge conditions. J. Geophys. Res.: Oceans 124 (7), 5220–5243.
Geological Survey, British, 2021. Carmarthen - geological Survey of England and Wales. Available: https://largeimages.bgs.ac.uk/iip/mapsportal.html?id=1001720. (Accessed 8 July 2021).
Gilby, B.L., Weinstein, M.P., Baker, R., Cebrian, J., Alford, S.B., Chelsky, A., Colombano, D., Connolly, R.M., Currin, C.A., Feller, I.C., Frank, A., 2021. Human actions alter tidal marsh seascapes and the provision of ecosystem services. Estuar. Coast 44 (6), 1628–1636.
Goslin, J., Clemmensen, L.B., 2017. Proxy records of Holocene storm events in coastal barrier systems: storm-wave induced markers. Quat. Sci. Rev. 174, 80–119.
Gray, J., Jones, S.R., Smith, A.D., 1995. Discharges to the environment from the Sellafield site, 1951-1992. J. Radiol. Prot. 15 (2), 99.
Haigh, I.D., Wadey, M.P., Wahl, T., Ozsoy, O., Nicholls, R.J., Brown, J.M., Horsburgh, K., Gouldby, B., 2016. Spatial and temporal analysis of extreme sea level and storm surge events around the coastline of the UK. Sci. Data 3 (1), 1–14.
Hawkes, A.D., Horton, B.P., 2012. Sedimentary record of storm deposits from hurricane Ike, Galveston and san Luis Islands, Texas. Geomorphology 171, 180–189.
Horsburgh, K., Horritt, M., 2006. The Bristol Channel floods of 1607–reconstruction and analysis. Weather 61 (10), 272–277.
Horton, B.P., Rossi, V., Hawkes, A.D., 2009. The sedimentary record of the 2005 hurricane season from the Mississippi and Alabama coastlines. Quat. Int. 195 (1–2), 15–30.
Horton, B.P., Shennan, I., Bradley, S.L., Cahill, N., Kirwan, M., Kopp, R.E., Shaw, T.A., 2018. Predicting marsh vulnerability to sea-level rise using Holocene relative sea-level data. Nat. Commun. 9 (1), 1–7.
Hughes, Z.J., FitzGerald, D.M., Wilson, C.A., Pennings, S.C., Więski, K., Mahadevan, A., 2009. Rapid headward erosion of marsh creeks in response to relative sea level rise. Geophys. Res. Lett. 36 (3), 1–5.
Kirwan, M.L., Megonigal, J.P., 2013. Tidal wetland stability in the face of human impacts and sea-level rise. Nature 504 (7478), 53–60.
Kirwan, M.L., Temmerman, S., Skeehan, E.E., Guntenspergen, G.R., Fagherazzi, S., 2016 Mar. Overestimation of marsh vulnerability to sea level rise. Nat. Clim. Change 6 (3), 253–260.
Kylander, M.E., Ampel, L., Wohlfarth, B., Veres, D., 2011. High-resolution X-ray fluorescence core scanning analysis of Les Echets (France) sedimentary sequence: new insights from chemical proxies. J. Quat. Sci. 26 (1), 109–117.
Leonardi, N., Ganju, N.K., Fagherazzi, S., 2016. A linear relationship between wave power and erosion determines salt-marsh resilience to violent storms and hurricanes. Proc. Natl. Acad. Sci. 113 (1), 64–68.
Leonardi, N., Carnacina, I., Donatelli, C., Ganju, N.K., Plater, A.J., Schuerch, M., Temmerman, S., 2018. Dynamic interactions between coastal storms and salt marshes: a review. Geomorphology 301, 92–107.
Liu, K.B., McCloskey, T.A., Bianchette, T.A., Keller, G., Lam, N.S., Cable, J.E., Arriola, J., 2014. Hurricane Isaac storm surge deposition in a coastal wetland along Lake Pontchartrain, southern Louisiana. J. Coast Res. 70 (10070), 266–271.
Lowe, J.A., Bernie, D., Bett, P., Bricheno, L., Brown, S., Calvert, D., Clark, R., Eagle, K., Edwards, T., Fosser, G., Fung, F., 2018. UKCP 18 Science Overview Report. Met Office Hadley Centre, Exeter, UK, pp. 2–15.
Löwemark, L., Chen, H.F., Yang, T.N., Kylander, M., Yu, E.F., Hsu, Y.W., Lee, T.Q., Song, S.R., Jarvis, S., 2011. Normalizing XRF-scanner data: a cautionary note on the interpretation of high-resolution records from organic-rich lakes. J. Asian Earth Sci. 40 (6), 1250–1256.
Lyddon, C., Knight, P., Leonardi, N., Brown, J., Plater, A., 2017. Flood hazard sensitivity to storm surge-high water concurrence in a hyper-tidal estuary. Coastal Dynam. Conf. 268–279.
Modern-Era retrospective analysis for research and Applications. Version 2. 2021. *Average Weather in Pembroke.* Available: https://weatherspark.com/y/36256/Average-Weather-in-Pembroke-United-Kingdom-Year-Round. Last accessed 16th March 2021.
Möller, I., Kudella, M., Rupprecht, F., Spencer, T., Paul, M., Van Wesenbeeck, B.K., Wolters, G., Jensen, K., Bouma, T.J., Miranda-Lange, M., Schimmels, S., 2014. Wave attenuation over coastal salt marshes under storm surge conditions. Nat. Geosci. 7 (10), 727–731.
Morris, R.L., Konlechner, T.M., Ghisalberti, M., Swearer, S.E., 2018. From grey to green: efficacy of eco-engineering solutions for nature-based coastal defence. Global Change Biol. 24 (5), 1827–1842.
Moskalewicz, D., Szczuciński, W. and Mroczek, P., (in press). Characterization of storm surge deposits along the shore of the Gulf of Gdańsk (Baltic Sea) applying heavy mineral analysis. Quat. Int., 1-12.
National Oceanographic Centre, 2021a. POLTIPS-3-Coastal Tidal Software. https://noc.ac.uk/business/marine-data-products/coastal. (Accessed 14 February 2020).
National Oceanographic Centre, 2021b. Chart Datum & Ordnance Datum. Available: https://www.ntslf.org/tides/datum. (Accessed 21 June 2021).
National Tidal Sea Level Facility, 2021. Tides and Storm Surges. Available. https://ntslf.org/storm-surges. (Accessed 15 October 2021).

Otvos, E.G., 2011. Hurricane signatures and landforms—toward improved interpretations and global storm climate chronology. Sediment. Geol. 239 (1–2), 10–22.
Palmer, M., Howard, T., Tinker, J., Lowe, J., Bricheno, L., Calvert, D., Edwards, T., Gregory, J., Harris, G., Krijnen, J., Pickering, M., 2018. UKCP 18 Marine Report. Met Office Hadley Centre, Exeter, UK, pp. 10–55.
Pannozzo, N., Leonardi, N., Carnacina, I., Smedley, R., 2021. Salt marsh resilience to sea-level rise and increased storm intensity. Geomorphology 389, 107825.
Pendleton, L., Donato, D.C., Murray, B.C., Crooks, S., Jenkins, W.A., Sifleet, S., Craft, C., Fourqurean, J.W., Kauffman, J.B., Marbà, N., Megonigal, P., 2012. Estimating global "blue carbon" emissions from conversion and degradation of vegetated coastal ecosystems. PLoS One 7 (9), e43542.
Phillips, M., Jones, H., Pontee, N., Williams, P., 2012. Three Rivers estuarine complex (14). Lavernock Point to St Ann's Head SMP2 1–2.
Pilarczyk, J.E., Dura, T., Horton, B.P., Engelhart, S.E., Kemp, A.C., Sawai, Y., 2014. Microfossils from coastal environments as indicators of paleo-earthquakes, tsunamis and storms. Palaeogeogr. Palaeoclimatol. Palaeoecol. 413, 144–157.
Poo, M.C.P., Yang, Z., Dimitriu, D., Qu, Z., Jin, Z., Feng, X., 2021. Climate Change Risk Indicators (CCRI) for Seaports in the United Kingdom, 205. Ocean & Coastal Management, 105580.
Port of Milford Haven, 2016. Milford haven waterway. Available: https://www.mhpa.co.uk/uploads/Marine_docs/P9_single_5year_recreation_plan.indd.pdf. (Accessed 14 March 2021).
Prahalad, V.N., Kirkpatrick, J.B., Mount, R.E., 2012. Tasmanian coastal saltmarsh community transitions associated with climate change and relative sea level rise 1975–2009. Aust. J. Bot. 59 (8), 741–748.
Pye, K., Blott, S.J., 2009. Coastal processes and shoreline behaviour of estuary dominated systems in Swansea bay and Carmarthen bay. Report prepared on behalf of Halcrow Group Ltd., 15, pp. 11–13. Swindon, by K. Pye Associates, Crowthorne, 3–4.
Resources Wales, Natural, 2020. Flood and coastal erosion risk management in Wales, 2016- 2019 Flood Coastal Erosion Risk Manag. Wales 3, 2–4.
Rupprecht, F., Möller, I., Paul, M., Kudella, M., Spencer, T., Van Wesenbeeck, B.K., Wolters, G., Jensen, K., Bouma, T.J., Miranda-Lange, M., Schimmels, S., 2017. Vegetation-wave interactions in salt marshes under storm surge conditions. Ecol. Eng. 100, 301–315.
Schlichting, R.B., 2000. Establishing the inundation distance and overtopping height of paleotsunami from the late-Holocene geologic record at open-coastal wetland sites, central Cascadia margin. Portland State University Journal 112 (3), 45–49.
Schwalm, C.R., Glendon, S., Duffy, P.B., 2020. RCP8. 5 tracks cumulative CO2 emissions. Proc. Natl. Acad. Sci. 117 (33), 19656–19657.
Shennan, I., Horton, B., 2002. Holocene land-and sea-level changes in Great Britain. J. Quat. Sci.: Publ. Quat. Res. Assoc. 17 (5-6), 511–526.
Shennan, I., Bradley, S.L., Edwards, R., 2018. relative sea-level changes and crustal movements in Britain and Ireland since the last glacial maximum. Quat. Sci. Rev. 188, 143–159.
Slingo, J., Belcher, S., Scaife, A., McCarthy, M., Saulter, A., McBeath, K., Jenkins, A., Huntingford, C., Marsh, T., Hannaford, J., Parry, S., 2014. The Recent Storms and Floods in the UK, pp. 2–26.
Spencer, T., Möller, I., Rupprecht, F., Bouma, T.J., Van Wesenbeeck, B.K., Kudella, M., Paul, M., Jensen, K., Wolters, G., Miranda-Lange, M., Schimmels, S., 2016. Salt marsh surface survives true-to-scale simulated storm surges. Earth Surf. Process. Landforms 41 (4), 543–552.
Swindles, G.T., Galloway, J.M., Macumber, A.L., Croudace, I.W., Emery, A.R., Woulds, C., Bateman, M.D., Parry, L., Jones, J.M., Selby, K., Rushby, G.T., 2018. Sedimentary records of coastal storm surges: evidence of the 1953 North Sea event. Mar. Geol. 403, 262–270.
Szczuciński, W., Kokociński, M., Rzeszewski, M., Chagué-Goff, C., Cachão, M., Goto, K., Sugawara, D., 2012. Sediment sources and sedimentation processes of 2011 Tohoku-oki tsunami deposits on the Sendai Plain, Japan—insights from diatoms, nannoliths and grain size distribution. Sediment. Geol. 282, 40–56.
Troels-Smith, J., 1955. Karakterisering af løse jordarter. Reitzel i Komm 9–32.
Tsompanoglou, K., Croudace, I.W., Birch, H., Collins, M., 2011. Geochemical and radiochronological evidence of North Sea storm surges in salt marsh cores from the Wash embayment (UK). Holocene 21 (2), 225–236.
Vinent, O.D., Johnston, R.J., Kirwan, M.L., Leroux, A.D., Martin, V.L., 2019. Coastal dynamics and adaptation to uncertain sea level rise: optimal portfolios for salt marsh migration. J. Environ. Econ. Manag. 98, 102262.
Wadey, M.P., Haigh, I.D., Brown, J.M., 2014. A century of sea level data and the UK's 2013/14 storm surges: an assessment of extremes and clustering using the Newlyn tide gauge record. Ocean Sci. 10 (6), 1031–1045.
Weltje, G.J., Tjallingii, R., 2008. Calibration of XRF core scanners for quantitative geochemical logging of sediment cores: theory and application. Earth Planet Sci. Lett. 274 (3–4), 423–438.
Weltje, G.J., Bloemsma, M.R., Tjallingii, R., Heslop, D., Röhl, U., Croudace, I.W., 2015. Prediction of geochemical composition from XRF core scanner data: a new multivariate approach including automatic selection of calibration samples and quantification of uncertainties. In: Micro-XRF Studies of Sediment Cores. Springer, Dordrecht, pp. 507–534.
Wentworth, C.K., 1922. A scale of grade and class terms for clastic sediments. J. Geol. 30 (5), 377–392.
Westlake, J.A., 2019. Meteotsunami: the AD 1607 Bristol channel flood. Emporium Lincoln 1 (2).
Williams, H.F., 2009. Stratigraphy, sedimentology, and microfossil content of Hurricane Rita storm surge deposits in southwest Louisiana. J. Coast Res. 25 (4), 1041–1051.
Williams, H.F., 2010. Storm surge deposition by hurricane Ike on the McFaddin national wildlife Refuge, Texas: implications for paleotempestology studies. J. Foraminiferal Res. 40 (3), 210–219.
Williams, H.F.L., Flanagan, W.M., 2009. Contribution of Hurricane Rita storm surge deposition to long-term sedimentation in Louisiana coastal woodlands and marshes. J. Coast Res. 1671–1675.
Williams, S.P., Goff, J.R., Sale, F., Ah Kau, J., Prasetya, G., Davies, T.R., Cheung, K.F., Wilson, T., 2011. Sands of Time: evidence for palaeotsunamis and/or palaeostorms in Samoa, and what this means for tsunami risk reduction. In: Proceedings of the Samoa National Environment Forum, pp. 15–25.
Woodroffe, S.A., Long, A.J., 2009. Salt marshes as archives of recent relative sea level change in West Greenland. Quat. Sci. Rev. 28 (17–18), 1750–1761.
Woodroffe, Barlow, Shennan, I., Long, A.J., Horton, B.P. (Eds.), 2015. Handbook of Sea-Level Research. John Wiley & Sons, pp. 176–177.
Zedler, J.B., 2010. How frequent storms affect wetland vegetation: a preview of climate-change impacts. Front. Ecol. Environ. 8 (10), 540–547.